

Degradation of cationic red X-GRL by electrochemical oxidation on modified PbO₂ electrode

Minghua Zhou^{a,b,*}, Jianjian He^a

^a Department of Environmental Science, Zhejiang University, Hangzhou 310028, China

^b Department of Chemical and Biomolecular Engineering, Sydney University, NSW 2006, Australia

Received 26 May 2007; received in revised form 21 August 2007; accepted 22 August 2007

Available online 25 August 2007

Abstract

This work investigated the degradation of an azo dye, cationic red X-GRL, by electrochemical oxidation on a novel PbO₂ anode modified by fluorine resin. The influences of treatment time, electrolyte concentration, current density, temperature and initial dye concentration on the color and COD removal were critically examined. This process showed a high current efficiency and competitive energy consumption for effective treatment of dye wastewater containing a certain salt content. In the investigated electrolyte concentrations, high salt content exhibited insignificant promotion on the color and COD removal but favored the decrease of energy consumption. During treatment, the current efficiency decreased but the energy consumption increased with treatment time; thus, this method was more suitable for the pretreatment of high-concentrated azo dye wastewater. Based on the degradation intermediates identification, a simplified degradation pathway for cationic red X-GRL was proposed.

© 2007 Elsevier B.V. All rights reserved.

Keywords: Electrochemical oxidation; Cationic red X-GRL; Azo dye; PbO₂ electrode; Degradation mechanism

1. Introduction

Azo dyes are typical pollutants found in many important industries such as textile, food colorants, printing and cosmetic manufacturing. It is estimated that approximately 800,000 t of dyes are produced annually worldwide and about 50% of them are azo dyes [1]. Effluents refractory to conventional treatments cause severe environmental problems due to the characteristics of strong color, high chemical oxygen demand (COD) and low biodegradability. Therefore, the treatment of these wastewaters is becoming a matter of great concern in sound and cost-effective technologies development to reach related standards before being discharged to the environment.

In recent years, advanced electrochemical oxidation processes (AOPs) for the destruction of wastewater containing toxic or biorefractory organic compounds have attracted ever-increasing interests due to their easy applicability to automation,

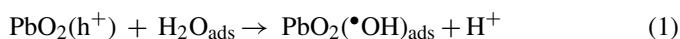
high efficiency and environmental compatibility [2–4]. The effective and economical performance of the process is dependent on electrode materials [5], and generally the non-active electrodes such as PbO₂ and SnO₂ exhibit a better performance for organic pollutants degradation than that of the active ones [6]. Several researchers have studied the azo dye degradation by electrochemical oxidation through optimization of operating parameters using various anodes including active carbon fiber (ACF) [7], Pt [8], RuO₂ [9], SnO₂ [10], PbO₂ [11] and diamond electrode [12,13]. Mohan et al. carried out the electro-oxidation of acid blue 113 using a RuO₂ electrode with the current efficiency of 0.2–0.4 and energy consumption of 61.3–131.0 kWh/kg COD [9]. Similar results were observed in their another work on acid violet 12, where the COD removal was no more than 35%, and the current efficiency was less than 0.4 for initial dye concentration of 140 mg/L [10]. Cañizares et al. used a relatively expensive diamond anode for electrochemical oxidation of azo dyes, but observed a low average current efficiency less than 0.2, and concluded the technique uneconomical for complete degradation [14]. Fernandes et al. used boron doped diamond (BDD) electrode to degrade C.I. acid orange 7, although high COD removal was achieved for initial dye concentration of 360 mg/L, long degradation time (>6.6 h)

* Corresponding author at: Department of Environmental Science, Zhejiang University, Hangzhou 310028, China. Tel.: +86 571 88273090; fax: +86 571 88273693.

E-mail address: skynumen@yahoo.com (M. Zhou).

was required due to the small electrode area of 10 cm² [13]. In summary, the performances on dye removal on these electrodes are not so satisfactory due to low current efficiency or small electrode area or expensive cost on electrode. Therefore, the exploration for good performance using novel electrodes which are relatively cheap and easy to fabricate large electrode area for environmental application seems to be essential.

In our previous work, a novel β -PbO₂ anode modified by fluorine resin with large electrode area (>250 cm²) was developed for phenolic wastewater treatment [15–17]. It was found that the electrode modification greatly improved the electrode life against wastewater, the electrochemical activity for organic pollutants degradation and the electrochemical stability. Phenol of initial concentration of 10 mM could be completely decomposed in 2.5 h at a current density of 12.5 mA/cm². And the organic pollutants degradation on this anode was proved to be a free-radical mechanism where hydroxyl radical (\bullet OH) formed as follows:



So in the present work, the objective was to investigate the feasibility of this electrode for the anodic degradation of azo dye using cationic red X-GRL as a model pollutant. Such a dye was chosen because it was widely used in textile, plastic and varnish industries and hardly biodegradable by conventional biological processes [18]. The influences of parameters such as current, temperature, supporting electrolyte and initial dye concentration were investigated to increase our understanding of this process involved the novel anode. Further, taking account for the facts that most of investigation paid attention to the optimization on color and COD removal while less information was provided for the degradation pathway or intermediates formation, the degradation intermediates was identified to elucidate the dye degradation pathway, which would help to gain some insight into this electrochemical oxidation process.

2. Experimental

2.1. Materials and chemicals

The dye used in the present work was purified from industrial cationic red X-GRL (Jin-jiang chemical dyestuff Co. Ltd., China) by extraction with methanol at 50 °C to reach the purity of 99.5% (the structure can be seen in Fig. 7). The synthetic wastewater was prepared by the purified dye and an inert electrolyte sodium sulfate which was one of the most common salts used for the dyeing process excepting NaCl.

2.2. Equipments and procedures

The experiments were carried out in a 2 L cylindrical stainless autoclave. The anode used here was a novel β -PbO₂ anode (\varnothing 45 mm \times 200 mm) modified with fluorine resin, which was located in the centre of the reactor. The anode

preparation procedures were principally including chemical deposition, α -PbO₂ preliminary deposition and β -PbO₂ deposition. More details of the anode preparation and its electrochemical characteristics were given in our previous work [15]. The current density calculated in the present work was based on the effective anode area of 250 cm². The cathode was a stainless steel net (grid 1 mm \times 1 mm) which was attached to the inert wall of the reactor and concentric with the anode with an electrode gap of about 4 cm. The solution of wastewater (1.3 L) was fed into the reactor, and when it reached the desired temperature, the experiments started, maintaining current constantly at the chosen level with only minor adjustments of the applied voltage. During each run, the wastewater was stirred at suitable speed (300 rpm) to maintain reactions kinetically controlled, and samples were taken from the sampling port for analysis at appropriate intervals. The analysis was determined triplicately with relative error within 3%.

2.3. Analysis

Dye concentration was analyzed spectrophotometrically by measuring the absorbance of the remaining dye at maximum wavelength 530 nm on a UV–vis spectrophotometer (Techcomp 8500, China).

The COD was measured by the standard method (closed reflux/photometry) [19]. The COD or color removal efficiency (η) was calculated by the following formula:

$$\eta = \frac{A_0 - A_t}{A_0} \times 100\% \quad (2)$$

where A_0 is the COD or absorbance of initial dye concentration and A_t is the COD or the remaining dye concentration at given time t .

The average current efficiency (ACE) was calculated by the following [14]:

$$\text{ACE} = \frac{(\text{COD}_0 - \text{COD}_t)FV}{8It} \times 100\% \quad (3)$$

where COD_0 and COD_t are the chemical oxygen demand at initial time and the given time t (g O₂/L), respectively, I the current (A), F the Faraday constant (96,487 C/mol), t the treatment time (s) and V is the volume of the solution (L).

The energy consumption (EC) was calculated by the following definition,

$$\text{EC} = \frac{UIt}{3.6(\text{COD}_0 - \text{COD}_t)V} \quad (4)$$

where U is the voltage applied (V), other parameters are as defined as before.

The degradation intermediates were analyzed using a trace 2000 GC/MS system (Trace 2000, ThermoQuest, USA) with HP-5 capillary column (30 m \times 0.32 mm, film thickness 0.25 μ m). The base temperature of the right SSL method was set at 260 °C, the oven temperature was initially at 50 °C, rising at 15 °C/min to a final temperature of 250 °C. The concentration of NO₂⁻ or NO₃⁻ was detected by ion chromatograph

(Techcomp 1000, China) with the mobile phase of sodium carbonate (1.8 mM) and sodium bicarbonate (1.7 mM) at the flow rate 1.0 mL/min.

3. Results and discussions

3.1. Effects of operating parameters

3.1.1. Effect of degradation time

Fig. 1a shows the time dependence of color, COD removal and pH variation. The color removal was higher than the COD removal, indicating that the structure of cationic red X-GRL especially the chromophore was broken and some acidic intermediates were produced, which could also be proved by the drop of the solution pH from the original 5.0 to final 3.27 after treated 240 min. At that time, the color removal reached 87.4% and simultaneously the COD removal reached 36.3%. Both the color and COD removal increased with treatment time and no obvious decay trends were observed, indicating that they could be further removed if given much more time. However, it was observed that the ACE decreased while the EC almost increased linearly with the COD removal (Fig. 1b), which might be related with the complexity of the intermediates formed, especially some hard-to-treatment products as disclosed in Section 3.2.

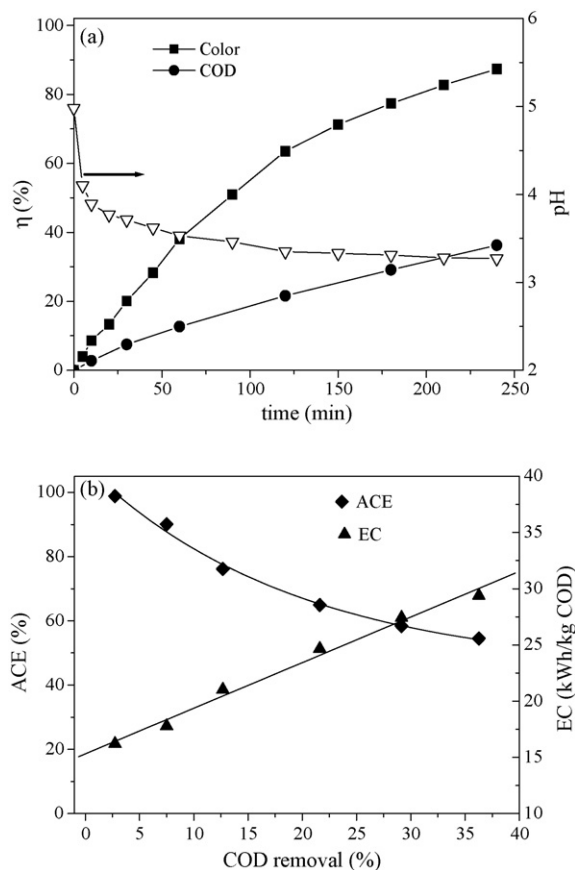


Fig. 1. (a) Effect of degradation time on color removal, COD removal and pH variation. (b) Variation of ACE and EC with COD removal. Conditions—pH: 5.0; cationic red X-GRL: 500 mg/L; current density: 2.0 mA/cm²; Na₂SO₄: 3 g/L; T: 25 °C.

This fact suggested that it would be better to pre-treat rather than mineralize the wastewater. At the initial stage, the ACE kept relatively high value of 98.8%, and it decreased with the increase of COD removal. Such a decay become insignificantly after the COD conversion of more than 20%, holding an ACE of 54.4% after treated 240 min. This decreasing trend with treatment time was similar with other reports [13,15], where they claimed that the generated organic acids were much more difficult to be decomposed and thus led to the relatively lower ACE. Compared the current efficiency with other works on azo dye degradation (less than 40%) [9,14], the present work showed a better performance, suggesting this electrochemical oxidation would be highly efficient using this novel anode. Though the EC increased with COD removal, it was no more than 30 kWh/kg COD for about 35% COD conversion, which was much lower than those other reports on azo dyes electrochemical oxidation [9]. Further, it was reported that an electrochemical process would be competitive if the EC was less than 40–50 kWh/kg COD comparing with other AOPs including ozonation [20]. This fact confirmed that the electrochemical oxidation on this electrode was one of the most promising pre-treatment techniques for azo dye.

3.1.2. Effect of electrolyte concentration

It is important to investigate the effect of electrolyte since actual wastewater usually contains certain amount of salts. Fig. 2 shows the effect of Na₂SO₄ concentration on color, COD removal and EC variation. It was observed that the Na₂SO₄ concentration within the investigated ranges appeared to be no difference on color and COD removal. According to the definition, the ACE for different Na₂SO₄ concentrations should also be insignificant because the applied currents were the same. However, it was found that the EC decreased dramatically with the increase of salt concentration, but further enlarged salt concentration beyond 3.0 g/L seemed to be of no considerable reduction on EC. When the Na₂SO₄ concentration was 0.5 g/L, the EC was as high as 44.4 kWh/kg COD, and when Na₂SO₄ concentration increased to 3 g/L, it dropped to 24.7 kWh/kg COD. This trend could be explained by the decrease of voltage, where the voltage applied was 7.68 V at Na₂SO₄ concentration of 0.5 g/L, and it

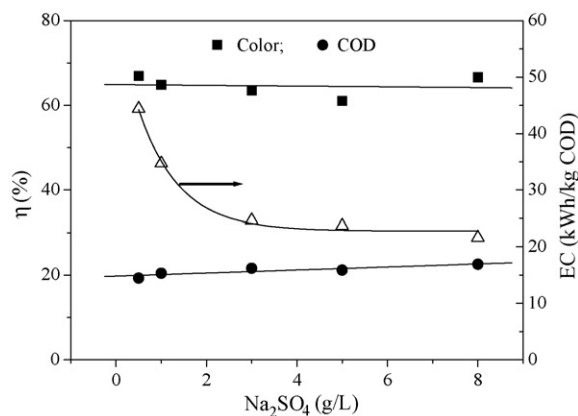


Fig. 2. Effect of Na₂SO₄ concentration on color, COD removal and EC variation. Conditions—pH: 5.0; cationic red X-GRL: 500 mg/L; current density: 2.0 mA/cm²; T: 25 °C; treated time: 120 min.

Table 1
The effect of current density on color and COD removal, ACE and EC

Current density (mA/cm ²)	Color (%)	COD (%)	ACE (%)	EC (kWh/kg COD)
0.8	43.3	13.0	97.5	12.4
2.0	63.6	21.6	64.9	24.7
4.8	87.1	38.2	47.8	45.6

Conditions—pH: 5.0; cationic red X-GRL: 500 mg/L; Na₂SO₄: 3 g/L; T: 25 °C; treated time: 120 min.

dropped to 4.78 V for the one of 3 g/L. These results indicated that a minimum amount of salt was required to start the degradation and high salt improved the treatment cost-effectiveness. Therefore, this process was supposed to be cost-effective for the treatment of wastewater containing a certain salt content.

3.1.3. Effect of current density

Table 1 shows the effect of current density on color and COD removal, ACE and EC. Obviously, high current density promoted the color and COD removal, which was similar with literature [15]. This result might be due to the generation rate of hydroxyl radical increased with current density, which eventually enhanced the dye degradation. At current density 0.8 mA/cm², the color removal was only 43.3%, while at current density 4.8 mA/cm², it was 87.1%. Simultaneously, the COD removal increased from 13.0 to 38.2%. The considerable promotion on performance indicated that current density was one of the key parameters determined the removal efficiency. However, the ACE decreased with the increase of current density, indicating that an increase in the current density led to a less efficient process. At time 120 min, the ACE for 0.8 mA/cm² was 97.5%, but at current density 4.8 mA/cm², it was only 47.8%. Such a decrease in the efficiency might be explained by the favor of anodic side reactions including oxygen evolution at elevated currents. As a consequence, the EC increased from 12.4 to 45.6 kWh/kg COD. These outcomes supported that at a low current density the performance would be cost-effective but need long treatment time, while at a high current density it was of highly efficient but costly. Therefore, according to the removal efficiency and current efficiency, the current density of 2.0 mA/cm² would be a good choice, where the color and COD removal and ACE would be relatively high, while EC would be affordable.

3.1.4. Effect of temperature

Fig. 3 shows the effect of temperature on color removal. As can be seen, an increase in the temperature leads to a more efficient process. The color removal rate increased significantly from temperature 15 °C, but when the temperature above 25 °C the effect was not so obvious. It was observed that when treated 120 min the color removal at the temperature of 15 and 25 °C was 24.3 and 63.6%, respectively, but when the temperature further increased to 60 °C, it only increased to 79.8%. This effect might be explained that high temperature promoted not only the dye degradation but also the generation of some hard-to-treatment intermediates, which resulted in competitive reactions among color removal and intermediates degradation, and thus led to

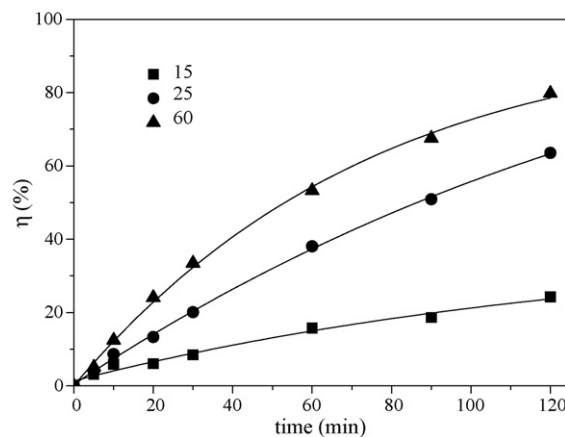


Fig. 3. Effect of temperature on color removal. Conditions—pH: 5.0; cationic red X-GRL: 500 mg/L; current density: 2.0 mA/cm²; Na₂SO₄: 3 g/L.

the enhancement on color removal was not so sensitive at high temperature of 60 °C.

3.1.5. Effect of initial dye concentration

Fig. 4 shows the effect of initial cationic red X-GRL concentration on color removal. When the initial concentration was 300 mg/L, the color removal was 68.9% within 120 min. With the increase of the dye concentration, the color removal percentages decreased to 18.4% for that of 2000 mg/L. This might be explained that the ratio of hydroxyl radical to dye concentration decreased with the increase in initial concentration. Although the color removal percentage decreased with initial concentration, the absolute removal amount increased. For example, when cationic red X-GRL concentration increased from 300 to 2000 mg/L, the removal amount increased from 206.7 to about 368.0 mg/L. This also confirmed by the increase of ACE and the decrease of EC at treated time 60 min (inset figure). For the initial concentration of 300 mg/L, the ACE and EC were about 62.7% and 28.3 kWh/kg COD, respectively, while for the one of 2000 mg/L, the ACE and EC were about 89.8% and 17.8 kWh/kg COD, respectively. Though a higher initial concen-

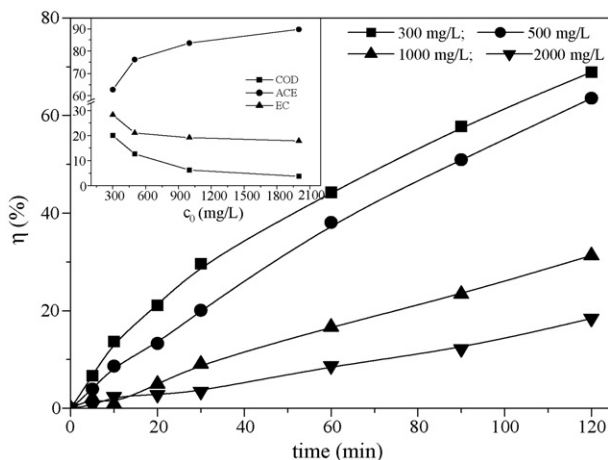


Fig. 4. Effect of initial dye concentration on color and COD removal. Conditions—pH: 5.0; Na₂SO₄: 3 g/L; current density: 2.0 mA/cm²; T: 25 °C.

tration led to a lower COD removal, taking account for the facts that the ACE and EC for initial concentration 500–2000 mg/L changed little, the COD removal would be increased if given much longer time. Therefore, this process seemed to be a good alternative for high-concentrated dye wastewater pretreatment.

3.2. Possible degradation mechanism

The absorption spectra of cationic red X-GRL degradation at typical time were investigated, as shown in Fig. 5. It can be observed that before treatment cationic red X-GRL is characterized by one main bond in the visible region with the peak absorbance at 530 nm, and the other two bonds in the ultraviolet region situated at around 280–290 nm and 240–250 nm. Different structural groups in the dye molecules have unique absorbance peak, and the main conjugates of cationic red X-GRL include azo linkage ($-\text{N}=\text{N}-$) and benzene ring. The chromophore containing azo bond has absorption in the visible region, which is ascribed to the absorption of the $n \rightarrow \pi^*$ transition related to the $-\text{N}=\text{N}-$ group. The benzene ring has absorption in ultraviolet region (240–250 nm), which is recognized to the absorption of the $\pi \rightarrow \pi^*$ transition. It was found that the absorbency of the remaining solution at visible light region decreased quickly, while simultaneously the absorbency at UV region increased, indicating that azo bond was destroyed and many degradation intermediates containing benzene ring generated. Accompanying the breakage of azo group, the absorbance at 280–290 nm was observed to be decreased, and that at 240–250 nm also increased a little.

To further explore the possible degradation mechanism, the degradation intermediates of cationic red X-GRL have been detected by GC/MS as shown in Fig. 6, and the main identified intermediates are listed in Table 2. The main degradation intermediates identified were *N*-phenylmethane-benzenamine (M1, relative abundance 100%), benzaldehyde (M2, 13%), and *N*-methyl-aniline (M3, 2%).

Based on the above degradation trend and the identified products, a simplified degradation pathway was proposed, as shown

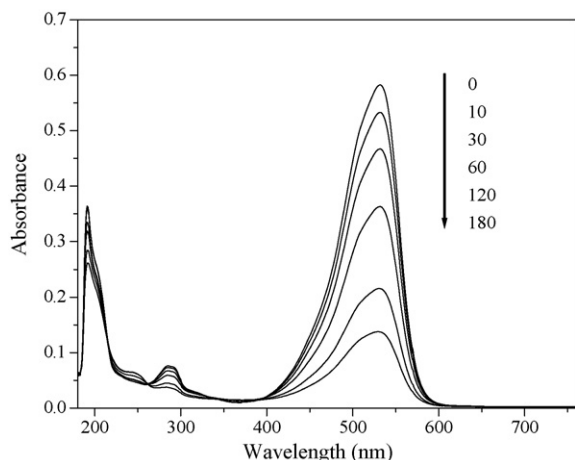


Fig. 5. Typical UV-vis spectra for cationic red X-GRL degradation by electrochemical oxidation.

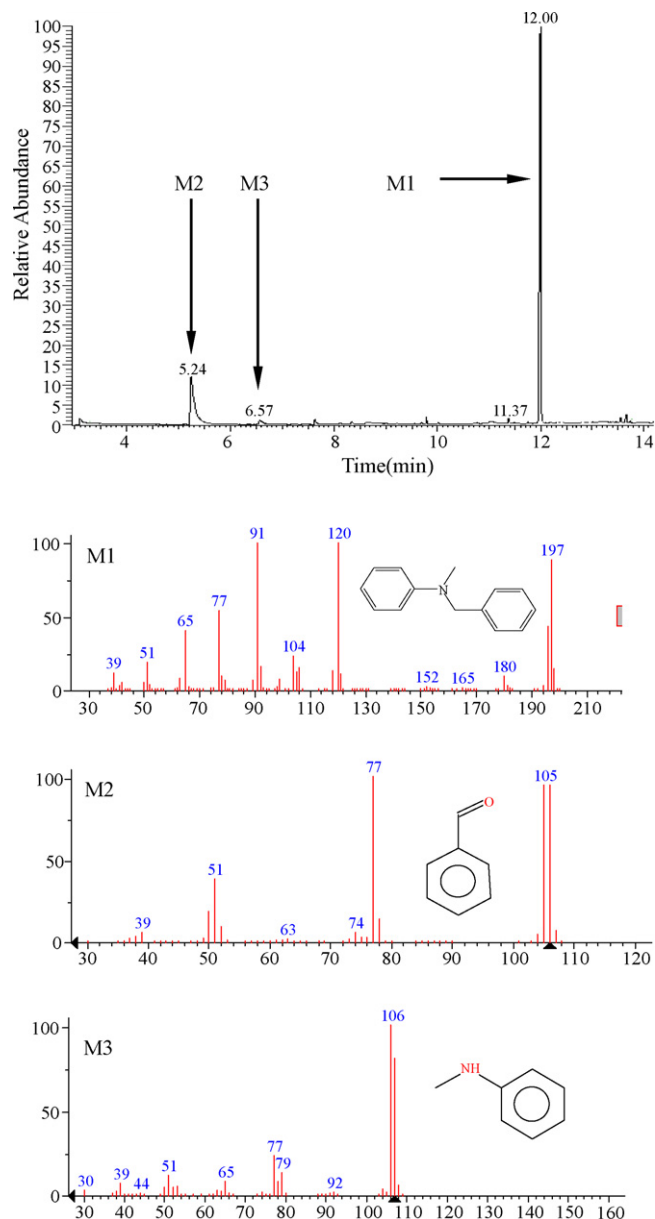


Fig. 6. GC/MS spectra of cationic red X-GRL by electrochemical oxidation.

in Fig. 7. The breakage of the azo bond would be the initial step of dye degradation, which led to the rapid removal of color. In the bond ($-\text{C}-\text{N}=\text{N}-$), the length of the bond of C(5)–N(6), N(6)–N(7) and N(7)–C(8) is 1.456, 1.362 and 1.404 Å, respectively, which indicated C(5)–N(6) would be the first potential broken bond among the three as for stability. The radical would attack this site and result in the release of nitrogen element and the formation of 2,4-dimethyl-2,4-dihydro-[1,2,4]triazol-3-one, which was identified in our previous work [18] though it might be missed in the analysis in the present work. However, it was confirmed that NO_2^- was not detected in the solution, while NO_3^- was very low (below 2 mg/L), which was much less than the theoretical calculation from the breakage of azo bond. In literatures, it was reported a degradation pathway for azo dye through the formation of molecular nitrogen [21]. In

Table 2
The main degradation intermediates of cationic red X-GRL

Code	t_R (min)	m/z	Molecular formula	Name	Structure
M1	12.0	197	$C_{14}H_{15}N$	<i>N</i> -phenylmethylene-benzenamine	
M2	5.24	106	C_7H_6O	Benzaldehyde	
M3	6.57	106	C_7H_8N	<i>N</i> -methyl-aniline	

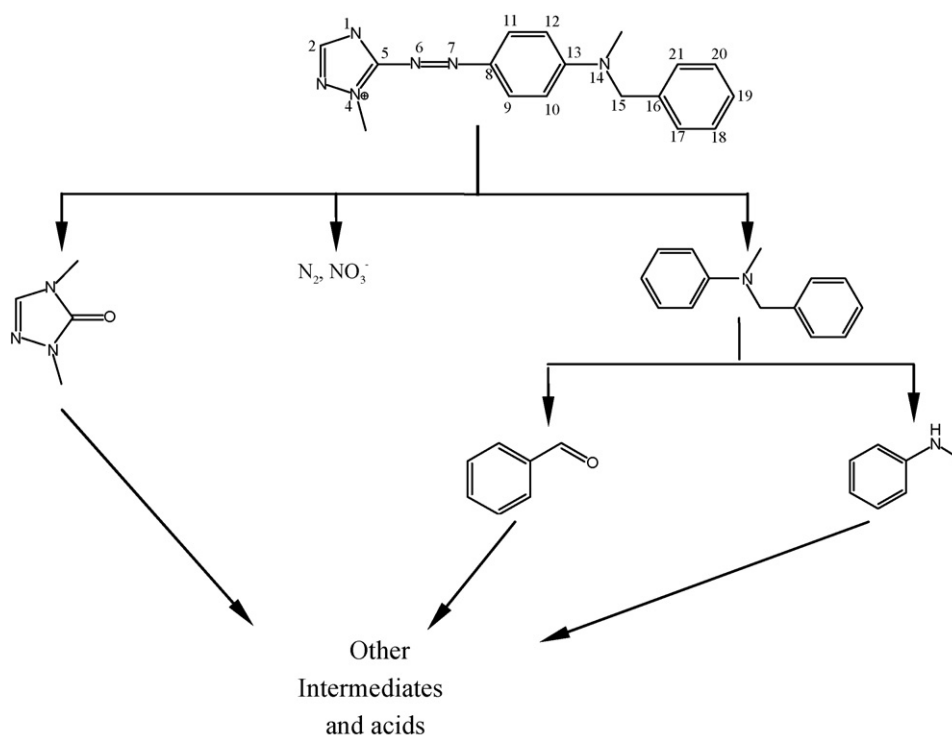


Fig. 7. Possible degradation pathway for cationic red X-GRL by electrochemical oxidation.

the present work, we deduced that the degradation might also proceed in this way. The breakage of azo group from the parent substance would result in the formation of *N*-phenylmethylene-benzenamine-diazeno radical, which would be unstable and then turned into *N*-phenylmethylene-benzenamine (M1) by release of molecular nitrogen. After the breakage of the azo dye to form M1, the hydroxyl radical attack would lead to the broken down of N(14)–C(15), which led to the formation of M2 and M3. These products would be further degraded to light molecule intermediates and organic acids as confirmed by the drop of the solution pH. Due to the relatively higher color removal and lower COD removal, it could be deduced that the decolorization of azo bond breakage was relatively easy but the further degradation intermediates to organic acids would be rather difficult.

4. Conclusions

The following conclusions can be drawn from the work described here.

- (1) The color and COD removal was significantly affected by the current density, temperature and initial dye concentration. At low current density, the performance would be cost-effective but need long treatment time, while at high current density it was of high efficiency but costly. So that, current density of 2.0 mA/cm^2 would be a good choice. The removal rate increase with the raise of temperature but decreased with the enhancement of initial dye concentration. The color and COD removal seemed to be independent with electrolyte concentrations, but the

energy consumption decreased with the increase of salt concentration.

- (2) Both the color and COD removal increased with treatment time and no obvious decay trends were observed, and high current efficiency (>50%) was achieved but decreased with time. Though the energy consumption increased with COD removal, it was not more than 30 kWh/kg COD for about 35% COD conversion, indicating that this method was cost-effective for the pretreatment of high-concentrated dye wastewater containing a certain salt content.
- (3) The main degradation intermediates identified were *N*-phenylmethylen-benzenamine, benzaldehyde and *N*-methyl-aniline. Based on the identified products, a possible degradation pathway was proposed. It disclosed that the breakage of azo group was relatively easy while difficult to be further degraded to organic acids, which well explained the color removal was quite rapid while COD removal was relatively difficult.

Acknowledgements

The project was supported by the National Natural Science Foundation of China (nos. 20306027 and 20676121), the Analysis and Detection Fund of Zhejiang Province (04173) and Natural Science Foundation of Zhejiang Province (no. Y504129) and Pao's Scholarship.

References

- [1] H. Zollinger, Color Chemistry—Synthesis, Properties and Applications of Organic Dyes and Pigments, VCH Publishers, New York, 1991.
- [2] K. Rajeshwar, J.G. Ibanez, G.M. Swain, Electrochemistry and environment, *J. Appl. Electrochem.* 24 (1994) 1077–1109.
- [3] Ch. Comminellis, Electrocatalysis in the electrochemical conversion/combustion of organic pollutants for waste water treatment, *Electrochim. Acta* 39 (1994) 1857–1862.
- [4] M.H. Zhou, Z.C. Wu, D.H. Wang, Electrocatalytic degradation of phenol in acidic and saline wastewater, *J. Environ. Sci. Heal. A.* 37 (2002) 1263–1275.
- [5] R. Kotz, S. Stucki, B. Caecer, Electrochemical waste water treatment using high overvoltage anode. Part I. Physical and electrochemical properties of SnO₂ anodes, *J. Appl. Electrochem.* 21 (1991) 14–21.
- [6] P. Cañizares, F. Martinez, M. Diaz, J. Garcia-Gomez, M.A. Rodrigo, Electrochemical oxidation of aqueous phenol wastes using active and nonactive electrodes, *J. Electrochem. Soc.* 149 (2002) D118–D124.
- [7] J.P. Jia, J. Yang, J. Liao, W.H. Wang, Z.J. Wang, Treatment of dyeing wastewater with ACF electrodes, *Water Res.* 33 (1999) 881–884.
- [8] M.A. Sanromán, M. Pazos, M.T. Ricart, C. Cameselle, Electrochemical decolourisation of structurally different dyes, *Chemosphere* 57 (2004) 233–239.
- [9] N. Mohan, N. Balasubramanian, V. Subramanian, Electrochemical treatment of simulated textile effluent, *Chem. Eng. Technol.* 24 (2001) 749–753.
- [10] N. Mohan, N. Balasubramanian, In situ electrocatalytic oxidation of acid violet 12 dye effluent, *J. Hazard. Mater.* 136 (2006) 239–243.
- [11] H.S. Awad, N.A. Galwa, Electrochemical degradation of acid blue and basic brown dyes on Pb/PbO₂ electrode in the presence of different conductive electrolyte and effect of various operating factors, *Chemosphere* 61 (2005) 1327–1335.
- [12] X.M. Chen, G.H. Chen, P.L. Yue, Anodic oxidation of dyes at novel Ti/B-diamond electrodes, *Chem. Eng. Sci.* 58 (2003) 995–1001.
- [13] A. Fernandes, A. Morão, M. Magrinho, A. Lopes, I. Goncalves, Electrochemical degradation of C.I. acid orange 7, *Dyes Pigments* 61 (2004) 287–296.
- [14] P. Cañizares, A. Gadri, J. Lobato, B. Nasr, R. Paz, M.A. Modrigo, C. Saez, Electrochemical oxidation of azoic dyes with conductive-diamond anodes, *Ind. Eng. Chem. Res.* 45 (2006) 3468–3473.
- [15] M.H. Zhou, Q.Z. Dai, L.C. Lei, C. Ma, D.H. Wang, Long life modified lead dioxide anode for organic wastewater treatment: electrochemical characteristics and degradation mechanism, *Environ. Sci. Technol.* 39 (2005) 363–370.
- [16] M.H. Zhou, L.C. Lei, The role of activated carbon on the removal of *p*-nitrophenol in an integrated three-phase electrochemical reactor, *Chemosphere* 65 (2006) 1197–1203.
- [17] M.H. Zhou, L.C. Lei, An improved UV/Fe³⁺ process by combination with electrocatalysis for *p*-nitrophenol degradation, *Chemosphere* 63 (2006) 1032–1040.
- [18] Q.Z. Dai, M.H. Zhou, L.C. Lei, Wet electrolytic oxidation of X-GRL, *J. Hazard. Mater.* 137 (2006) 1870–1874.
- [19] APHA, AWWA, WEF, Standard Method for the Examination of Water and Wastewater, 19th ed., APHA, Washington, DC, 1995.
- [20] S. Stucki, R. Kotz, B. Carcer, W. Stuer, Electrochemical waste-water treatment using high overvoltage anodes. 2. Anode performance and applications, *J. Appl. Electrochem.* 21 (1991) 99–104.
- [21] J.T. Spadaro, L. Isabelle, V. Renganathan, Hydroxyl radical mediated degradation of azo dyes: evidence for benzene generation, *Environ. Sci. Technol.* 28 (1994) 1389–1393.